Supporting Information

Evaporation-Induced Particle Microseparations inside Droplets Floating on a Chip

Suk Tai Chang and Orlin D. Velev*

* E-mail: odvelev@unity.ncsu.edu

Four supplementary movies visualizing the processes are provided (in Windows AVI format):

1. Confocal_reconstruction_rotating.avi

Confocal microscopy 3D reconstruction of the distribution of the particles in an evaporating droplet containing 0.2 wt% of 1 μm fluorescent latex. The top half of the droplet is originally viewed from the side. The angle of view is then digitally "rotated" so it ends up in view from the top. Nearly all particles are concentrated in the apex of the droplet.

2. Side_view_flow.avi

The movie shows the circular flow in an evaporating droplet viewed from the side. The flow is in the form of a single roll cell. The droplet contains 0.41 wt% of 4.9 μm latex spheres. The observation is carried out with 0.7-4.5×zoom stereomicroscope

3. Top_view_flow.avi

One-directional flow in an evaporating droplet from top-down view. The circular patch in the middle is the island of particles collected in the top droplet portion. The flow suggests a no-slip boundary condition in this region. The droplet contains 4.1 wt% of 4.9 μm latex. The movie is taken with an Olympus BX-61 optical microscope focused on the top of the droplet.

4. Initial_top_flow.avi

Top-down view of an evaporating droplet in the initial stages of the process, before particles have collected to immobilize the top surface. The flow in the top of the droplets moves to the left. The flow further down (seen here on the sides) moves to the right. Similar pattern is predicted by the 2D simulation of the initial flow pattern shown in the Figure below.

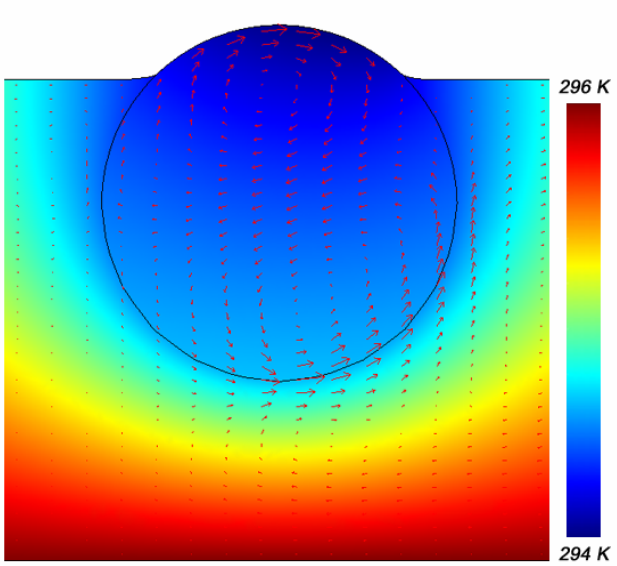

Supplementary Figure 1. Simulation for the temperature distribution and velocity profile at an initial stage of drying of a droplet with relative humidity 55% and ambient temperature 23°C. The top water/air surface is not immobilized by a particle layer and the boundary condition there is $\tau_{water} - \tau_{air} = \nabla \sigma_{water/air} \cdot \mathbf{t}$. The other boundary conditions are the same as those described in the manuscript. The velocity vector magnitudes are represented by the lengths of the arrows. The liquid on the top moves in one direction, while the liquid further down moves in the opposite direction. The flows are broadly similar to the experimentally observed ones before the droplet surface is immobilized by particle layers (see Movie 4). After particles accumulate in the top section they immobilize the surface and suppress the top vortex, leading to the flow pattern similar to the simulation in Figure 10.

Supplementary Table. Numerical values for the physical properties of the fluids at T = 23°C

Fluid	Density ρ (kg/m^3)	Viscosity η (kg/m s)	Thermal conductivity k (J/m s K)	Thermal diffusivity α (m^2/s)	Thermal expansion β (K^{-1})	Surface tension derivative at air/liquid interface $\lvert d\sigma/dT \rvert$ (N/m K)	Interfacial tension derivative at water/oil interface. $\lvert d\sigma/dT \rvert$ (N/m K)	Latent heat h_l (kJ/kg)
Water	1.0×10^3 [a]	0.94×10^{-3} [a]	0.604 [a]	1.449×10^{-7} [a]	0.236×10^{-3} [a]	$\sim1.5\times10^{-4}$ [c]	$\sim10^{-4}$ [e]	2442.5 [a]
Fluorinert oil FC-70	1.94×10^3 [b]	24×10^{-3} [b]	0.697 [b]	0.342×10^{-7} [b]	0.001 [b]	$\sim10^{-4}$ [d]		69 [b]

[a] Data from Ref. 54. [b] Data from the product information data sheet of Fluorinert oil FC-70. [c] Data from Ref. 19. [d] Data from Ref. 55. [e] No data found in literature, assumed to be approximately the same as the corresponding number of water/air interface